J|A|C|S COMMUNICATIONS

Published on Web 01/30/2007

Highly Efficient G-Quadruplex Recognition by Bisquinolinium Compounds

Anne De Cian,[‡] Elsa DeLemos,[†] Jean-Louis Mergny,[‡] Marie-Paule Teulade-Fichou,*[,†] and David Monchaud[†]

Laboratoire de Chimie des Interactions Moléculaires, Collège de France, CNRS UPR285, 75005 Paris, France, and Laboratoire de Biophysique, Muséum National d'Histoire Naturelle, USM503, INSERM U565 CNRS UMR 5153, 75005 Paris, France

Received October 13, 2006; E-mail: mp.teulade-fichou@college-de-france.fr

Trying to control and regulate the expression of genes is emerging as a very appealing anticancer strategy. Indeed, chemotherapy aiming at designing molecules able to interact with unusual structures of nucleic acids is currently subjected to a close examination.[1] In that sense, quadruplex−DNA is a particularly attractive high-order structure since it appears to be putatively present in pivotal genomic regions such as telomeres,[2] promoters of oncogenes, and most growth control genes.[3] Convincing reports on the efficiency of quadruplex interacting molecules as therapeutically active agents are beginning to appear in the literature.[4]

Thus, intensive investigations are currently oriented toward the design and development of new G-quadruplex ligands. Of particular interest are molecules with high quadruplex affinity that exhibit the ability to discriminate quadruplex−DNA from nucleus predominant duplex-DNA. Up to now, the leading G-quadruplex binder has been the natural product telomestatin.[5] Nevertheless, its total synthesis was achieved only very recently, and the complexity of the process renders its convenient exploitation difficult.[6] Recently, some of us reported on bisquinolinium compounds that exhibit exceptional affinity and selectivity for quadruplex-forming oligonucleotides.[4c,7] The anti-proliferative activity of these compounds has been demonstrated, as well as their preferential binding to telomeric regions of human chromosomes,[7b] thus providing new insights on quadruplex existence in vivo. These exciting results prompted us to develop the bisquinolinium family of compounds which was furthermore facilitated by a convenient and rapid synthetic access.

In the initial series, the two quinolinium moieties are connected through a 2,6-pyridodicarboxamide unit.[4c,7] This motif, well-known to adopt an internally organized H-bonded *syn*−*syn* conformation (Figure 1A),[8] was shown to be critical for quadruplex binding. Indeed, inversion of the amide connectivity leads to a loss of affinity (Supporting Information).[4c] This suggests that the central pyridodicarboxamide unit locks the ligand in a crescent-shaped conformation highly favorable for G-quartet overlap. On this basis, we reasoned that expanding the aromaticity of the central core without disrupting either the H-bonds network or modifying the cationic side-arm nature could result in improved recognition properties.

To this end, 6,6′-disubstituted-2,2′-bipyridine and 2,9-disubstituted-1,10-phenanthroline units that are also susceptible to be conformationally locked via H-bonding were considered as good candidates for replacing the pyridine central core. Ligands **1a**/**b** and **2a**/**b** (Figure 1B) were synthesized via straightforward three- and four-step procedures respectively, from inexpensive commercially available material (Supporting Information).

The ligand's ability to stabilize a quadruplex structure was evaluated by FRET experiments using the quadruplex-forming engineered oligonucleotide F21T (*FAM*-$G_3[T_2AG_3]_3$-*Tamra*), which

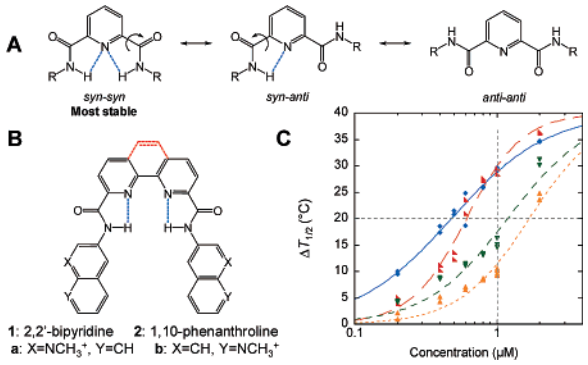

Figure 1. (A) Alternative conformations of pyridodicarboxamide unit (H-bonds appear as dotted lines). (B) Structure of **1a**/**b** and **2a**/**b** (with triflate as counterions). (C) Dose−response curves for FRET results ($\Delta T_{1/2}$) in function of ligand concentration for **1a** (green), **1b** (orange), **2a** (blue), and **2b** (red). The baseline ($\Delta T_{1/2}$ = 0 °C) was set at the melting temperature of the structure without ligand (48 °C).

mimics the human telomeric repeat (Supporting Information).[9] As shown in Figure 1C, compounds **2a**/**b** (blue/red curves) appear as remarkably strong quadruplex stabilizers, while more modest effects are obtained with **1a**/**b** (green/orange curves). Indeed, $\Delta T_{1/2}$ values at 1 μM dose of ligand (vertical gray line, Figure 1C) are significantly higher with **2a**/**b** ($\Delta T_{1/2(1\mu M)}$ = 29.7 and 28.5 °C, respectively) than with **1a**/**b** ($\Delta T_{1/2(1\mu M)}$ = 15.2 and 9.6 °C, respectively). Accordingly, the concentration required to achieve a $\Delta T_{1/2}$ value of 20 °C (horizontal gray line, Figure 1C) is also significantly lower with **2a**/**b** ($[conc]_{(\Delta T_{1/2}=20°C)}$ = 0.48 and 0.61 μM, respectively) than with **1a**/**b** ($[conc]_{(\Delta T_{1/2}=20°C)}$ = 1.19 and 1.69 μM, respectively).[10] Altogether, these data reflect a very high level of quadruplex stabilization for ligands **2** and represent a significant improvement as compared to the pyridine series. Interestingly, these results make this new series fully competitive with the high-affinity G-quadruplex binders such as telomestatin, extended acridines, and organometallic complexes all exhibiting $\Delta T_{1/2(1\mu M)} > 20$ °C.[10] Most important, the differences between the two series highlight that structural rigidity is a key parameter for quadruplex recognition, the free rotation around the biaryl axis of ligands **1** being responsible for the lower performance of this series.

To gain further insights into the intrinsic qualities of these ligands, competitive FRET experiments were performed in the presence of various amounts of 26 bp duplex-DNA (ds26, from 0 to 10 μM, Supporting Information).[11] Remarkably, the thermal stabilization induced by **2a**/**b** is only poorly affected (∼10% loss) by the presence of 10 molar equiv of ds26 (Figure 2A,B). This indicates that ligands **2** exhibit an exquisite quadruplex versus duplex selectivity, thus behaving similarly to telomestatin in the same conditions (Supporting Information).[12] Again, bipyridine derivatives **1** appear less competent since they are more sensitive

[†] Collège de France.
[‡] Muséum National d'Histoire Naturelle.

10.1021/ja067352b CCC: $37.00

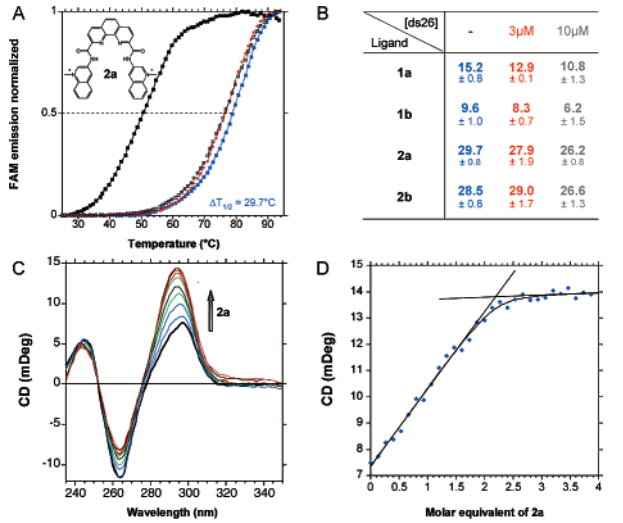

Figure 2. (A) FRET experiments carried out with **2a** and F21T without ligand (black) and with 1 μM **2a** in absence (blue) or presence of competitive duplex (ds26, 3 equiv (red) or 10 equiv (gray)). (B) FRET results ($\Delta T_{1/2}$, °C) for **1a**/**b** and **2a**/**b** (1 μM) in absence (blue) or presence of competitive ds26 (3 equiv (red) or 10 equiv (gray)). (C and D) CD titration of 22AG (3 μM in 10 mM lithium cacodylate, pH 7.2, 100 mM NaCl buffer) by increasing amounts of **2a**: (C) some CD spectra at 296 nm from the titration experiment; the arrow indicates the increasing amounts of ligand (from black to red curves: 0, 1.2, 2.4, 3.6, 4.7, 5.9, 7.1, 8.2, 9.4, and 10.9 μM); (D) CD signal as a function of **2a** molar equivalents (0.4 μM increments).

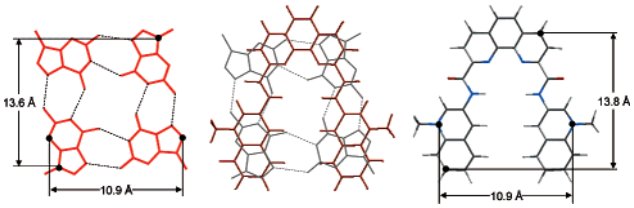

Figure 3. Selected dimensions of a G-quartet (left, determined from X-ray structure) and of **2a** (right, after molecular mechanics (MM2) calculations (Chem3D Ultra 8.0, CambridgeSoft Corp., MA)).

to the duplex competition (29 and 35% loss in stabilization for **1a**/**b**, respectively (Figure 2B).

To determine the stoichiometry of association of **2a** and G-quadruplexes, CD titrations were carried out using the 22AG sequence ($AG_3[T_2AG_3]_3$, in Na^+ buffer, Figure 2C and Supporting Information).[13] Analysis of the data indicates that the curve inflection occurs at ~2:1 ligand/quadruplex ratio (Figure 2D). This 2:1 stoichiometry is consistent with a binding mode based on the stacking of the ligand onto the two external G-quartets of the quadruplex (Supporting Information).

A close examination of the crystal structure of 22AG (1KF1, RCSB Protein Data Bank)[14] shows that a G-quartet can be considered as a square aromatic surface whose dimensions are closely related to that of **2a** (Figure 3 and Supporting Information). The strong stabilization properties of ligands **2** could thus originate in this accurate geometrical complementarity. Subsequently, the molecular size may be unfavorable for interaction with a classical base pair in duplex DNA,[1] resulting in the high preference for the quadruplex. Consequently, the molecular organization of the central core (internal H-bonds) and electronic/electrostatic properties (two quinolinium side arms) make phenanthroline bisquinolinium derivatives **2** perfectly fitted for the recognition of the quadruplex target.

Finally, the inhibitory properties of these ligands were evaluated via a classical TRAP assay (Supporting Information). However, preliminary data were obtained which suggest that inhibition measured by TRAP does not actually reflect telomerase inhibition but may result from an inhibition of the PCR amplification on quadruplex-prone motifs even though the internal PCR control (ITAS) is not affected (Supporting Information). Detailed explanations will be reported elsewhere. Nevertheless, the obtained results, among the best reported to date, represent a ~20-fold improvement as compared to the parent pyridine series[4c,7] and may reflect somehow the very good affinity of those ligands for quadruplex-prone motifs, confirming FRET melting results.

In conclusion, the present paper describes the quadruplex-binding properties of new members of the bisquinolinium family. Their easy synthetic access combined with exceptional quadruplex affinities and selectivities place these ligands among the most potent ones reported so far. Further in vitro evaluations are currently underway.

Acknowledgment. This work was supported by ARC (#3365) and E.U. FP6 "MolCancerMed" (LSHC-CT-2004-502943) grants. The authors gratefully thank Dr. P. Mailliet for helpful discussions.

Supporting Information Available: Synthesis and characterization of **1a**−**2b**; experimental procedures and additional FRET and CD data. This material is available free of charge via the Internet at http://pubs.acs.org.

References

(1) Wheelhouse, R. T.; Jennings, S. A.; Phillips, V. A.; Pletsas, D.; Murphy, P. M.; Garbett, N. C.; Chaires, J. B.; Jenkins, T. C. *J. Med. Chem.* **2006**, *49*, 5187.
(2) Neidle, S.; Parkinson, G. N. *Curr. Opin. Struct. Biol.* **2003**, *13*, 275.
(3) (a) Cogoi, S. C.; Xodo, L. E. *Nucleic Acids Res.* **2006**, *34*, 2536. (b) Dexheimer, T. S.; Sun, D.; Hurley, L. H. *J. Am. Chem. Soc.* **2006**, *128*, 5404. (c) Dai, J.; Dexheimer, T. S.; Chen, D.; Carver, M.; Ambrus, A.; Jones, R. A.; Yang, D. *J. Am. Chem. Soc.* **2006**, *128*, 1096. (d) Xu, Y.; Sugiyama, H. *Nucleic Acids Res.* **2006**, *34*, 949. (e) De Armond, R.; Wood, S.; Sun, D.; Hurley, L. H.; Ebbinghaus, S. W. *Biochemistry* **2005**, *44*, 16341. (f) Phan, A. T.; Kuryavyi, V.; Gaw, H. Y.; Patel, D. J. *Nat. Chem. Biol.* **2005**, *1*, 167. (g) Sun, D.; Guo, K.; Rusche, J. J.; Hurley, L. H. *Nucleic Acids Res.* **2005**, *33*, 6070. (h) Rankin, S.; Reszka, A. P.; Huppert, J.; Zloh, M.; Parkinson, G. N.; Todd, A. K.; Ladame, S.; Balasubramanian, S.; Neidle, S. *J. Am. Chem. Soc.* **2005**, *127*, 10584.
(4) (a) Burger, A. M.; Dai, F.; Schultes, C. M.; Reszka, A. P.; Moore, M. J. B.; Double, J. A.; Neidle, S. *Cancer Res.* **2005**, *65*, 1489. (b) Kim, M. Y.; Vankayalapati, H.; Shin-Ya, K.; Wierzba, K.; Hurley, L. H. *J. Am. Chem. Soc.* **2002**, *124*, 2098. (c) Pennarun, G.; Granotier, C.; Gauthier, L. R.; Gomez, D.; Hoffschir, F.; Mandine, E.; Riou, J.-F.; Mergny, J.-L.; Mailliet, P.; Boussin, F. *Oncogene* **2005**, *24*, 2917.
(5) (a) Shin-ya, K.; Wierzba, K.; Matsuo, K.-I.; Ohtani, T.; Yamada, Y.; Furihata, K.; Hayakawa, Y.; Seto, H. *J. Am. Chem. Soc.* **2001**, *123*, 1262. (b) Tahara, H.; Shin-ya, K.; Seimiya, H.; Yamada, H.; Tsuruo, T.; Ide, T. *Oncogene* **2006**, *25*, 1955. (c) Gomez, D.; O'Donohue, M. F.; Wenner, T.; Douarre, C.; Macadre, J.; Koebel, P.; Giraud-Panis, M. J.; Kaplan, H.; Kolkes, A.; Shin-ya, K.; Riou, J.-F. *Cancer Res.* **2006**, *66*, 6908.
(6) Doi, T.; Yoshida, M.; Shin-ya, K.; Takahashi, T. *Org. Lett.* **2006**, *8*, 4165.
(7) (a) Lemarteleur, T.; Gomez, D.; Paterski, R.; Mandine, E.; Mailliet, P.; Riou, J.-F. *Biochem. Biophys. Res. Commun.* **2004**, *323*, 802. (b) Granotier, C.; Pennarun, G.; Riou, L.; Hoffshir, F.; Gauthier, L. R.; De Cian, A.; Gomez, D.; Mandine, E.; Riou, J.-F.; Mergny, J.-L.; Mailliet, P.; Dutrillaux, B.; Boussin, F. D. *Nucleic Acids Res.* **2005**, *33*, 4182.
(8) Berl, V.; Huc, I.; Khoury, R. G.; Krische, M. J.; Lehn, J.-M. *Nature* **2000**, *407*, 720.
(9) Mergny, J.-L.; Maurizot, J.-C. *ChemBioChem* **2001**, *2*, 124.
(10) (a) Schultes, C. M.; Guyen, B.; Cuesta, J.; Neidle, S. *Bioorg. Med. Chem. Lett.* **2004**, *14*, 4347. (b) Moore, M. J. B.; Schultes, C. M.; Cuesta, J.; Cuenca, F.; Gunaratnam, M.; Tanious, F. A.; Wilson, W. D.; Neidle, S. *J. Med. Chem.* **2006**, *49*, 582. (c) Reed, J. E.; Arnal, A. A.; Neidle, S.; Vilar, R. *J. Am. Chem. Soc.* **2006**, *128*, 5992.
(11) Mergny, J.-L.; Lacroix, L.; Teulade-Fichou, M.-P.; Hounsou, C.; Guittat, L.; Hoarau, M.; Arimondo, P. B.; Vigneron, J. P.; Lehn, J.-M.; Riou, J.-F.; Garestier, T.; Hélène, C. *Proc. Natl. Acad. Sci. U.S.A.* **2001**, *98*, 3062.
(12) De Cian, A.; Guittat, L.; Shin-ya, K.; Riou, J.-F.; Mergny, J.-L. *Nucleic Acids Symp. Ser.* **2005**, *49*, 235.
(13) Allain, C.; Monchaud, D.; Teulade-Fichou, M.-P. *J. Am. Chem. Soc.* **2006**, *128*, 11890.
(14) Parkinson, G. N.; Lee, M. P. H.; Neidle, S. *Nature* **2002**, *417*, 876.

JA067352B

Highly Efficient G-Quadruplex Recognition by Bisquinolinium Compounds.

Anne De Cian,[‡] Elsa DeLemos,[†] Jean-Louis Mergny,[‡] Marie-Paule Teulade-Fichou,[*,†] and David Monchaud,[†]

Laboratoire de Chimie des Interactions Moléculaires, Collège de France, CNRS UPR285 & Laboratoire de Biophysique, Muséum National d'Histoire Naturelle, USM503, INSERM U565 CNRS-UMR 5153, 75005 Paris France.

Email : mp.teulade-fichou@college-de-france.fr

Supporting informations :

S1- Structures:

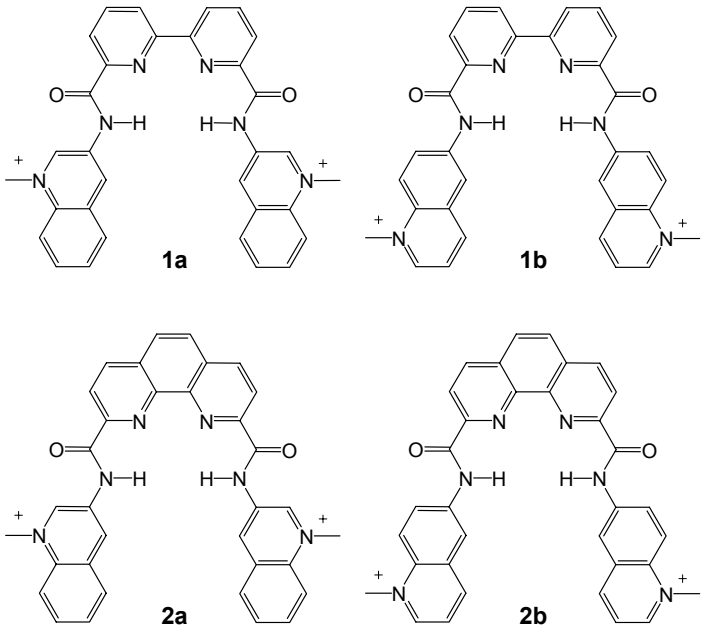

NB : For all compounds, the two counter-ions are $CF_3SO_3^-$.

S2- Synthesis of 1a-2b:

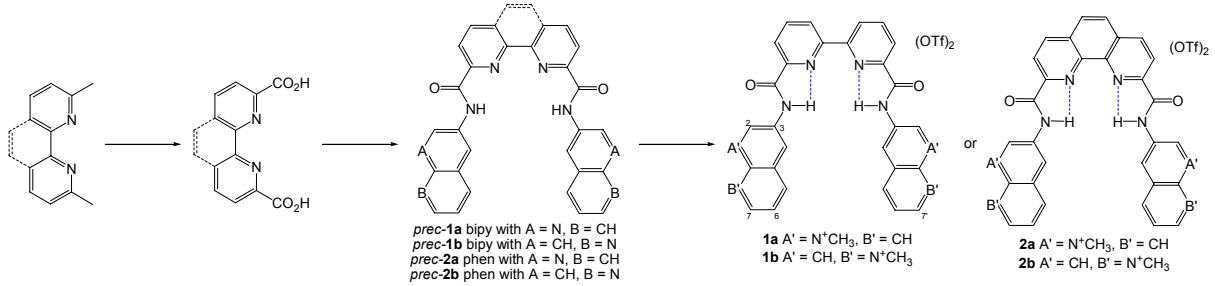

Reagents and conditions: (i) for bipyridine: $KMnO_4$, H_2O, 100°C, 2hrs, 40%; for phenantholine: SeO_2, dioxane, 100°C, 2hrs, 61% then HNO_3 (70%), 100°C, 3hrs, 76%; (ii) EDCI, HOAt, DMF, 23°C, 16hrs, 75-89%; (iii) MeOTf, DCE, 60°C, 16hrs, 50-86%. The internal N-H···N H-bonds are represented in blue. Carbon numbering for aminoquinoline is indicated on **1**; '*prec*-' stands for 'precursor of'.

Experimental part: the example of **2a**:

Step *i*-a: Selenium dioxide (4.0g, 36.0mmol, 5.0equiv.) is added to a solution of 2,9-dimethyl-1,10-phenanthroline (1.5g, 7.2mmol, 1.0equiv.) in dioxane (100mL) at room temperature. The reaction mixture is then heated to reflux under strong stirring for 2hours, and then allowed to cool to room temperature. The formed precipitated is collected and dried by several Et_2O washings. After removal of the solvent under reduced pressure, the crude material (1,10-phenanthroline-2,9-dicarbaldehyde) is obtained as a yellow powder (972mg, 61% chemical yield). **^{1}H-NMR** (300MHz, DMSO-d6) δ (ppm): 10.34 (s, 2H); 8.77 (d, *J*=8.1Hz, 2H); 8.28 (d, *J*=8.1Hz, 2H); 8.27 (s, 2H); **^{13}C-NMR** (75MHz, DMSO-d6) δ (ppm): 194.1; 152.6; 145.7; 138.9; 131.9; 129.7; 120.6; **M.p.** 230°C; **IR** (KBr) cm^{-1}: 2361 (C-H ald.); 2342 (C-H ald.); 1702 (C=O ald.).

Step *ii*-b: 1,10-phenanthroline-2,9-dicarbaldehyde (500mg, 2.1mmol, 1.0equiv.) is then stirred in a solution of HNO_3 (70%, 10mL) under reflux for 2 hours. After cooling to 0°C, slow addition of water (50mL) leads to the formation of a precipitate, which is collected and dried by several Et_2O washings. After removal of the solvent under reduced pressure, the crude material obtained was crystallised from methanol to give the 1,10-phenanthroline-2,9-dicarboxylic acid as a pale yellow powder (430mg, 76 %). **^{1}H-NMR** (300MHz, DMSO-d6) δ (ppm): 8.74 (d, *J*=8.1Hz, 2H); 8.42 (d, *J*=8.4Hz, 2H); 8.22 (s, 2H); **^{13}C-NMR** (75MHz, DMSO-d6) δ (ppm): 166.7; 148.6; 145.1; 138.7; 130.9; 128.8; 124.3; **M.p.** 239°C; **IR** (KBr) cm^{-1}: 3500 (O-H acid); 1718 (C=O acid); 1384 (O-H acid); 1292 (C-O acid).

Step *iii*: EDCI (150mg, 0.78mmol, 2.0equiv.) and HOAt (10mg, 0.074mmol, 0.2equiv.) are successively added to a solution of 1,10-phenanthroline-2,9-dicarboxylic acid (100mg, 0.37mmol, 1.0equiv.) and 3-aminoquinoline (113mg, 0.78mmol, 2.1equiv.) in DMF (10mL). The reaction mixture is then stirred at room temperature for 1 hour; the formed precipitated is collected, washed with a solution of $NaHCO_3$ (1%) and dried by several Et_2O washings. *Prec*-**2a** is obtained as a pale yellow solid (173mg, 89% chemical yield). **^{1}H-NMR** (300MHz, DMSO-d6) δ (ppm): 9.46 (s, 2H); 9.07 (s, 2H); 8.77-8.66 (m, 4H); 8.20 (s, 2H); 7.99 (m, 4H); 7.61 (m, 4H); **M.p.** <260°C ; **ESI-MS** (CH_2Cl_2/MeOH): m/z = 521 (100%; [*prec*-**2a**+H^+]);

Step *iv*: A solution of *prec*-**2a** (50mg, 0.096mmol, 1.0equiv.) in 1,2-dichloroethane (30mL) is heated to reflux under inert atmosphere. An excess of methyl trifluoromethanesulfonate is added (0.3mL, 2.65mmol, 27equiv.) and the reaction mixture is stirred overnight at reflux temperature. After cooling to room temperature, the formed precipitate is collected and dried by several Et_2O washings. **2a** is obtained as a pale yellow solid (40mg, 50% chemical yield).

S3- Characterisations of 1a-2b:

Ligand **2a:**
^{1}H-NMR (300MHz, DMSO-d6) δ (ppm): 12.2 (s, 2H); 10.3 (s, 2H); 9.93 (s, 2H); 8.99 (d, *J* = 8.4Hz, 2H); 8.78 (d, *J* = 8.4Hz, 2H); 8.56 (dd, *J* = 9.0, 3.6Hz, 2H); 8.40 (s, 2H); 8.26 (t, *J* = 7.8Hz, 2H); 8.09 (t, *J* = 7.8Hz, 2H); 4.68 (s, 6H);
^{13}C-NMR (75MHz, DMSO-d6) δ (ppm): 164.0; 148.8; 146.2; 140.1; 136.0; 135.2; 134.3; 133.0; 131.2; 130.8; 130.6; 129.5; 123.3; 122.6; 119.7; 114.6; 46.5;
M.p. >260°C ;
ESI-MS (MeOH): m/z = 275.1 (100%; [**2a**]/2);
HR-MS (MeOH): 550.2128 ($C_{34}H_{26}N_6O_2$, calc. 550.2117).

Ligand **2b:**
^{1}H-NMR (300MHz, DMSO-d6) δ (ppm): 12.1 (s, 2H); 9.45-9.31 (m, 4H); 9.12 (s, 2H); 8.92 (m, 4H); 8.70 (m, 4H); 8.33 (m, 2H); 8.19 (m, 2H); 4.72 (s, 6H);
^{13}C-NMR (75MHz, DMSO-d6) δ (ppm): 163.9; 149.4; 144.1; 139.8; 139.5; 135.9; 134.3; 130.8; 130.4; 129.1; 123.6; 122.8; 122.3; 120.8; 119.0; 117.6; 45.8;
M.p. >260°C ;
ESI-MS (MeOH): m/z = 275.1 (100%; [**2b**]/2);
HR-MS (MeOH): 550.2070 ($C_{34}H_{26}N_6O_2$, calc. 550.2117).

Ligand **1a:**
^{1}H-NMR (300MHz, DMSO-d6) δ (ppm): 11.6 (s, 2H); 10.1 (d, *J* = 2.1Hz, 2H); 9.66 (s, 2H); 9.38 (dd, *J* = 6.1, 2.1Hz, 2H); 8.55-8.41 (m, 6H); 8.24 (t, *J* = 7.5Hz, 2H); 8.10 (t, *J* = 7.8Hz, 2H); 4.75 (s, 6H);
^{13}C-NMR (75MHz, DMSO-d6) δ (ppm): 163.9; 154.1; 148.8; 146.0; 140.2; 136.1; 135.9; 132.8; 130.6; 130.4; 129.6; 126.2; 124.4; 123.6; 119.6; 46.4;
M.p. >260°C ;
ESI-MS (MeOH): m/z = 263.1 (100%; [**1a**]/2);
HR-MS (MeOH): 526.2092 ($C_{32}H_{26}N_6O_2$, calc. 526.2117).

Ligand **1b:**
^{1}H-NMR (300MHz, DMSO-d6) δ (ppm): 11.3 (s, 2H); 9.44-9.30 (m, 6H); 9.15 (s, 2H); 8.77-8.60 (m, 4H); 8.44-8.39 (m, 4H); 8.16 (dd, *J* = 8.4, 6.0Hz, 2H); 4.66 (s, 6H);
^{13}C-NMR (75MHz, DMSO-d6) δ (ppm): 163.9; 154.0; 149.4; 149.1; 146.9; 140.0; 139.5; 135.9; 131.7; 130.5; 125.8; 124.1; 122.9; 120.3; 118.5; 46.1;
M.p. >260°C ;
ESI-MS (MeOH): m/z = 263.1 (100%; [**1b**]/2);
HR-MS (MeOH): 526.2088 ($C_{32}H_{26}N_6O_2$, calc. 526.2117).

S4- FRET results with 1a-2b:

Ligand **2a** (internal reference: **EDL35**), **2b** (internal reference: **EDL39**), **1a** (internal reference: **EDL93**), **1b** (internal reference: **EDL95**); Duplicates at the same concentration are presented with the identical colour.

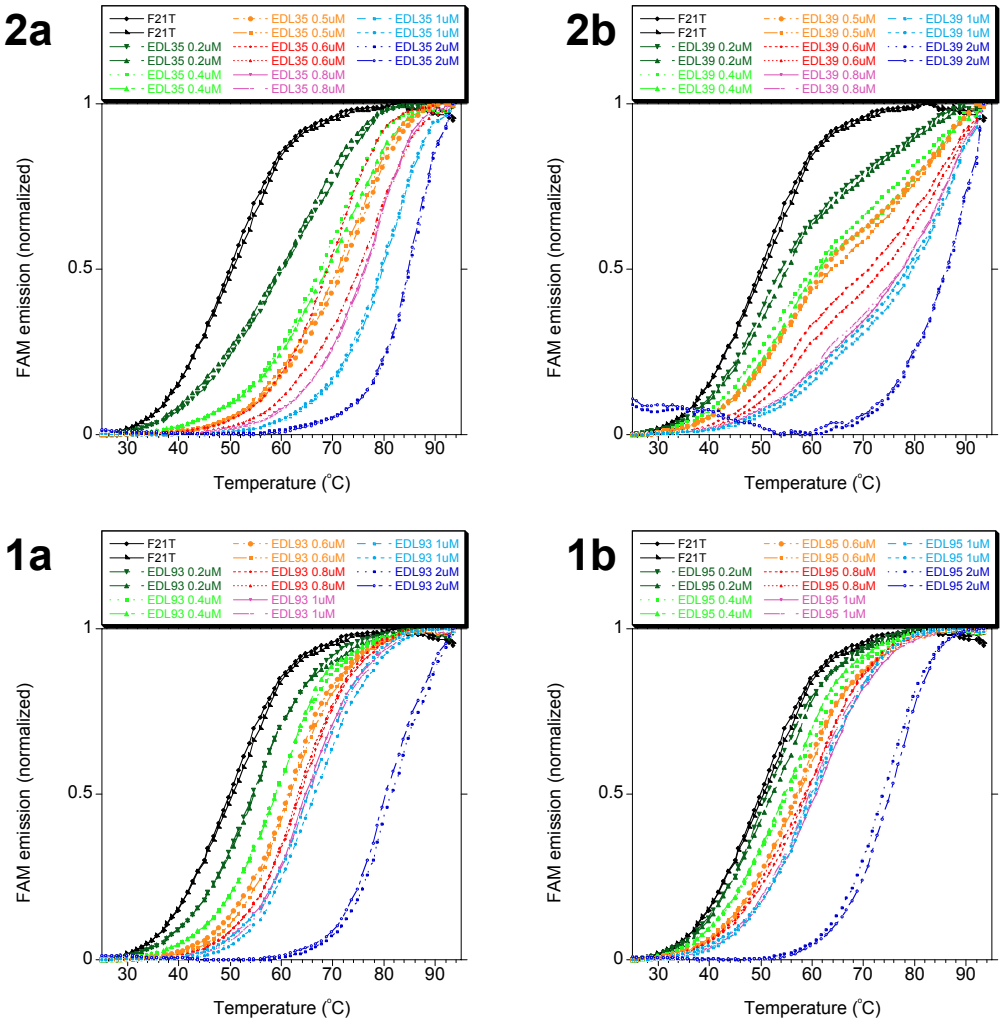

Competitive FRET with 0.5 or 1µM of compounds **1a-2b** and 0, 3µM and 10µM of duplex competitor ds26.

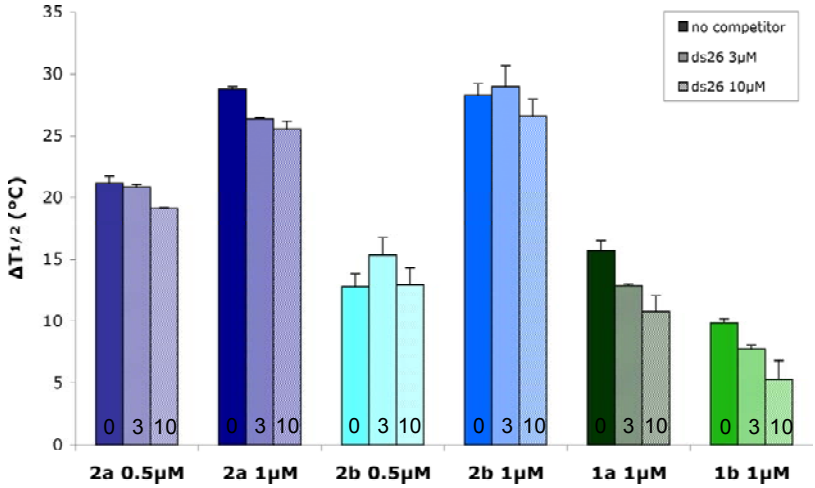

S5- FRET Protocol:

Labelled oligonucleotide is purchased from Eurogentec (Belgium); after an initial dilution at 100µM concentration in purified water, further dilutions are carried out in the relevant buffer.

FRET assay is performed as a high-throughput screen in a 96-well format, with F21T (*FAM*-$G_3[T_2AG_3]_3$-*Tamra*, with *FAM*: 6-carboxyfluorescein and *Tamra*: 6-carboxy-tetramehtylrhodamine). Fluorescence melting curves were determined with a Stratagene Mx3000P real-time PCR machine, using a total reaction volume of 25µL, with 0.2µM of tagged oligonucleotide in a buffer containing 10mM lithium cacodylate pH 7.2 and 100mM NaCl. After a first equilibration step at 25°C during 5 minutes, a stepwise increase of 1°C every minute for 71 cycles to reach 95°C was performed and measurements were made after each "cycle" with excitation at 492nm and detection at 516nm. The melting of the G-quadruplex was monitored alone or in the presence of various concentrations of compounds and/or of double-stranded competitor ds26 ($^{5'}$-CAATCGGATCGAATTCGATCCGATTG-$^{3'}$).

Final analysis of the data was carried out using Excel and Kaleida graph software. Emission of FAM was normalized between 0 and 1, and $T_{1/2}$ was defined as the temperature for which the normalized emission is 0.5. $\Delta T_{1/2}$ values are mean of 2 to 4 experiments ± standard deviation.

S6- FRET results with telomestatin:

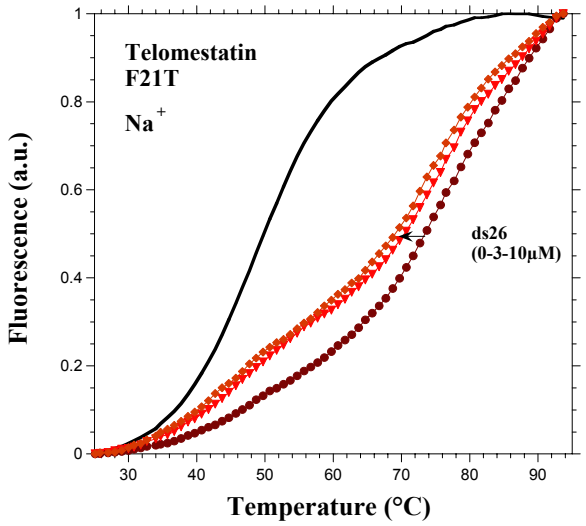

Competitive FRET with 1µM of telomestatin without (brown curve) or with 3 (red curve) or 10µM (orange curve) of duplex competitor ds26; these experiments is carried out in a sodium buffer. The stabilization obtained is the following: 23.6±0.3, 21.6±0.4 and 21.4±1.5°C for experiments with 0, 3 and 10µM of ds26.

The data and the full experimental details are reported in: De Cian, A.; Guittat, L.; Shin-ya, K.; Riou, J.-F.; Mergny, J.-L. *Nucleic Acids Symp. Series* **2005**, *49*, 235.

S7- **Inversion of amide connectivity** (Internal reference **EDL21**)**:**

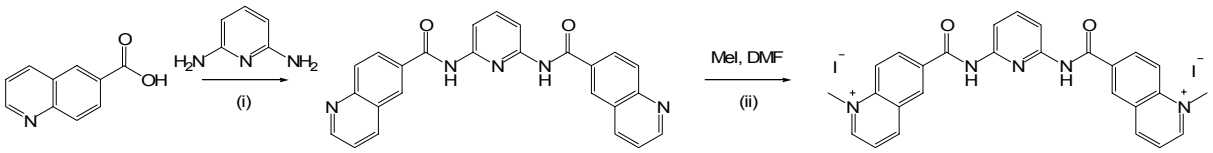

Step *i*: EDCI (972mg, 4.7mmol, 3.1equiv.) and HOAt (100mg, 0.72mmol, 0.47equiv.) are successively added to a solution of 6-quinolinecarboxylic acid (956mg, 5.52mmol, 3.1equiv.) and 2,6-diaminopyridine (200mg, 1.8mmol, 1.0equiv.) in DMF (40mL). The reaction mixture is then stirred at room temperature for 16hours. After removal of the solvent under reduced pressure, the residue is triturated in water and washed with Et_2O. After purification by column chromatography (silica gel, from DCM to 10% MeOH/DCM), neutral bisquinoline derivative is obtained as a pale yellow solid (43mg, 10% chemical yield). **R*f*** (DCM/MeOH 9:1) = 0.7; **^{1}H-NMR** (300MHz, DMSO-d6) δ (ppm): 12.9 (s, 2H); 10.8 (s, 2H); 9.03 (d, J = 2.7Hz, 2H); 8.73 (d, *J* = 9.0Hz, 2H); 8.30 (dd, *J* = 1.8, 8.4Hz, 2H); 8.14 (d, *J* = 8.7Hz, 2H); 7.97 (s, 3H); 7.66 (dd, *J* = 4.2, 8.4Hz, 2H); **^{13}C-NMR** (75MHz, DMSO-d6) δ (ppm): 166.0; 152.9; 151.0; 149.4; 140.5; 137.8; 132.3; 129.6; 129.5; 128.5; 127.5; 122.8; 111.7**; M.p.** >260°C.

Step *ii*: A solution of the previously prepared bisquinoline derivative (40mg, 0.095mmol, 1.0equiv.) in DMF (1mL) and MeI (5mL) is heated to reflux under inert atmosphere for 16 hours. After cooling to room temperature, the formed precipitate is collected and dried by several Et_2O washings. The amide-inversed bisquinolinium compound (**EDL21**) is obtained as an orange solid (48mg, 71% chemical yield). **^{1}H-NMR** (300MHz, DMSO-d6) δ (ppm): 11.2 (s, 2H); 9.59 (d, J = 6.0Hz, 2H); 9.38 (d, J = 8.1Hz, 2H); 9.09 (s, 2H); 8.76-8.63 (m, *4*H); 8.27 (d, *J* = 5.7Hz, 2H); 8.00 (m, 3H); 4.68 (s, 6H); **^{13}C-NMR** (75MHz, DMSO-d6) δ (ppm): 164.6; 154.9; 151.9; 150.7; 148.5; 140.0; 135.5; 134.2; 131.1; 129.0; 125.2; 120.2; 46.1; **M.p.** >260°C ; **EI-MS** (MeOH): m/z = 224.5 (100%; [**EDL21**]/2).

FRET results:

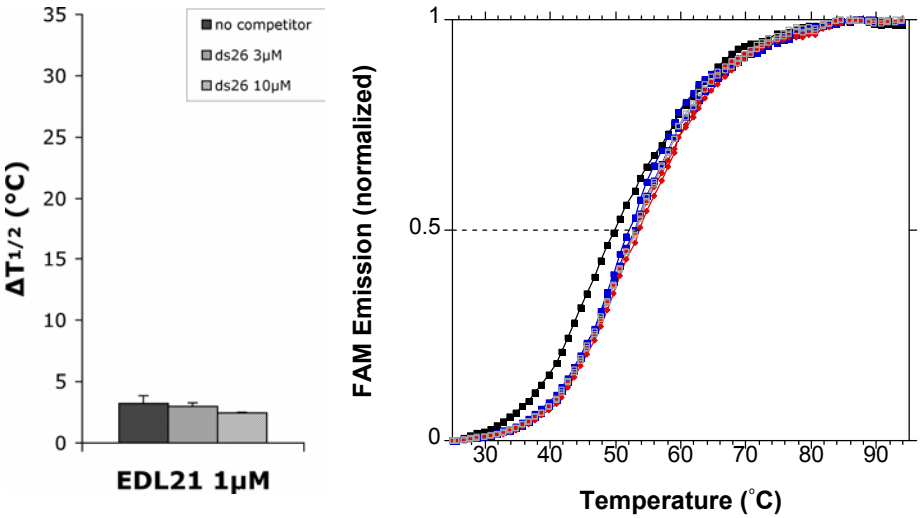

S8 **- CD titrations**:

Circular dichroism may be used to evidence the binding of **2a** to the human telomeric quadruplex in sodium (left) or potassium (right). Increasing amounts of **2a** lead to a progressive change in the spectra. Intensities at selected wavelengths *vs.* ligand concentration are shown in the central panels. A more dramatic change in the shape of the CD spectra is observed in K^+. This could be the result of a ligand-induced conformational change of the quadruplex: several quadruplex topologies have been reported for the human telomeric repeat in potassium, and the ligand may have different affinities for the various forms and shift the equilibrium towards a specific conformation. This conformational change may be kinetically forbidden (panel F): annealing the quadruplex in the presence of **2a** leads to a different spectra that adding the compound to the preformed quadruplex. Hence, the titration shown in panel B (and quantitated in panel D) does not reflect a thermodynamic equilibrium (binding of **2a** to the preformed quadruplex is fast, but the conversion into a different quadruplex conformation is very slow). Hence, the 4:1 binding stoichiometry deduced from the titration in panel D must be taken with caution. No such effect is obtained in sodium (panel E), in agreement with a simpler binding mode / single quadruplex conformation.

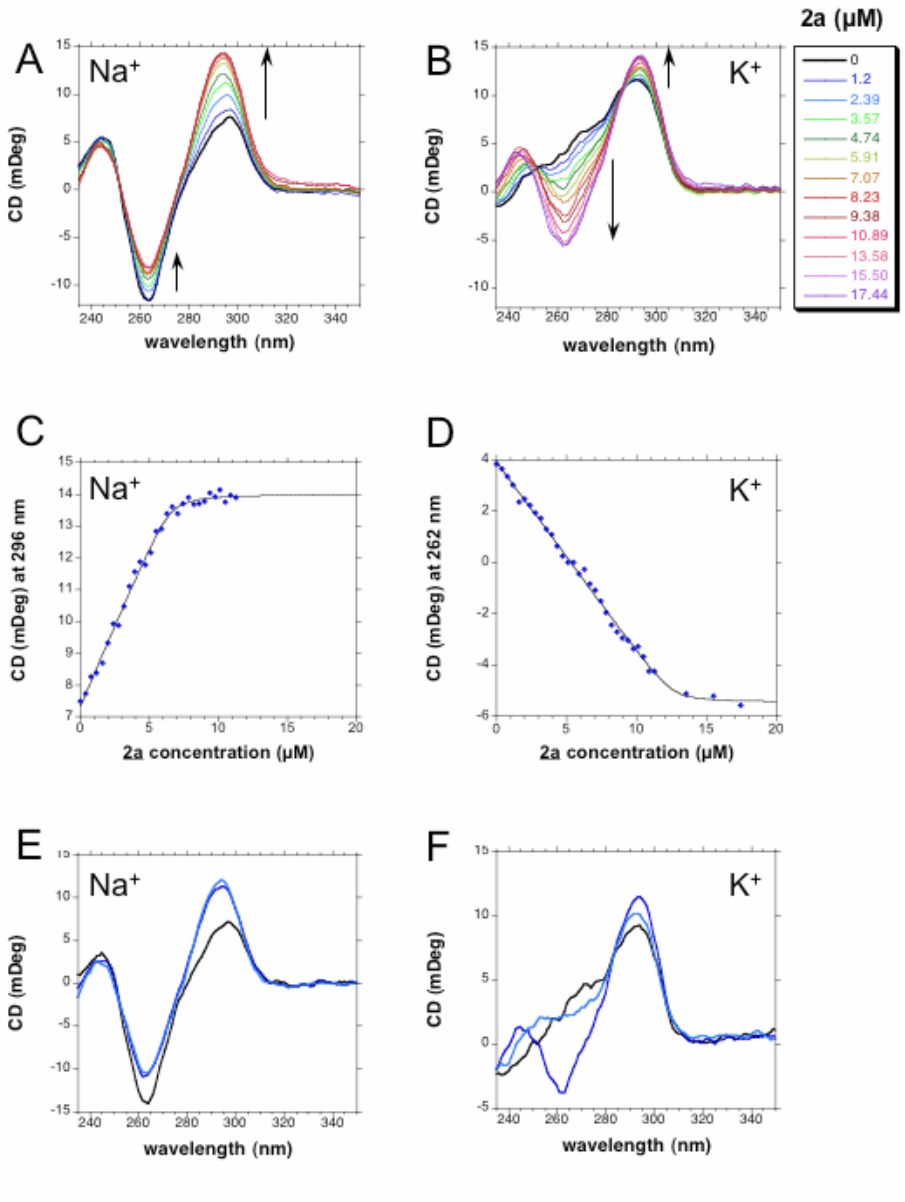

Figure Legend:

A-D: CD Titration : CD spectra of 22AG (3µM in 10 mM Lithium cacodylate pH 7.2, 100 mM NaCl (A) or KCl (B)) with increasing concentrations of **2a** (colour code shown on the right). The black curve stands for the oligonucleotide 22AG alone in both salt conditions. Arrows indicate the effects of increasing amounts of ligand on the CD signal. **C-D:** CD signal of 22AG complex with **2a** at 296nm in Na^+ buffer (C) or at 262 nm in K^+ buffer (D) as a function of **2a** concentration.

E-F: CD spectra of 22AG (3µM in 10 mM Lithium cacodylate pH 7.2, 100 mM NaCl (E) or KCl (F)) alone (black curves) or with 6µM of **2a** (blue curves) when the compound is added on the pre-annealed oligonuceotide (dark blue) or when the annealing is done in presence of the compound (light blue). Scans are performed in the same conditions than for CD titration.

Experimental procedure:

CD spectra were recorded on a JASCO-810 spectropolarimeter using 1 cm pathlength quartz cuvets in a reaction volume of 3ml. 22AG ([5'-$AG_3(T_2AG_3)_3$-3']) was prepared as a 3µM solution in 10mM lithium cacodylate pH 7.2, 100mM NaCl or KCl buffer and annealed by heating to 90°C for 2min, followed by a thermostated cooling to 20°C (at 10°C/min rate). Aliquots of 3µl of **2a** at 400µM (0.4µM increments) (in 10mM lithium cacodylate pH 7.2, 100mM NaCl or KCl buffer, 20% DMSO) were added to the 3ml of 22AG solution. Scans were performed at 20°C over a wavelength range of 235-350nm with a scanning speed of 200nm/min, a response time of 1s, 1nm pitch and 1nm bandwidth. A blank sample containing only buffer was substracted from the collected data. The CD spectra represent an average of two scans without any zero correction. Final analysis of the data was carried out using Excel and Kaleidagraph 3.6.2 software.

S9- Binding mode investigations:

To investigate the binding mode of **1a**-**2b**, competitive melting experiments have been performed using a non-loop containing tetramolecular G-quadruplex $[d(TG_5T)]_4$ as competitor.

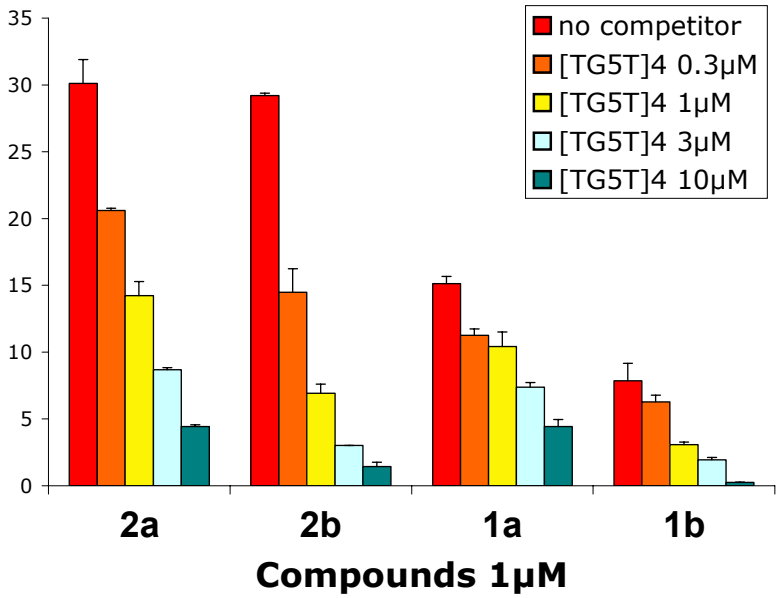

Competitive FRET with 1µM of **1a**-**2b** without (red) or with 0.3 (orange), 1 (yellow), 3 (blue) or 10µM (green bar) of tetramolecular quadruplex competitor $[d(TG_5T)]_4$.

In these conditions, a strong decrease in stabilization of 22AG was observed for the four ligands indicating that the ligands are easily displaced from the loop-containing quadruplex to the non-loop containing quadruplex. This demonstrates a strong binding of ligands **1** and **2** to the non loop containing G-quadruplex thus supporting that the binding mode is mainly based on stacking interaction with tetrads.

S10- UV-vis analysis of Bisquinolinium in solution:

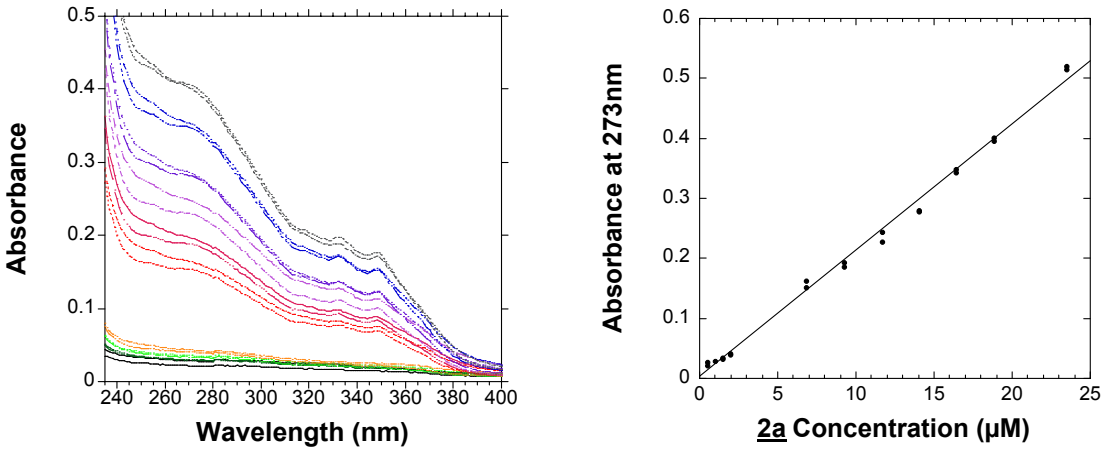

Concentration dependant UV-vis absorbance of compound **2a** has been recorded and shows that the variation follows the Beer-Lambert law. It is thus unlikely that the ligands do dimerize or self associate in absence of quadruplex.

S11- TRAP results:

Telomerase inhibition is classically evaluated in a TRAP assay. This assay involves a two-step procedure. A short oligonucleotide sequence is first extended by telomerase (from a crude human cell extract). Extension products are then amplified by PCR and revealed on a gel. Telomerase adds a 6 base-long motif, leading to a typical ladder. Various concentrations of drugs are tested in each lane. An internal control (ITAS) is provided to exclude non specific PCR inhibition.

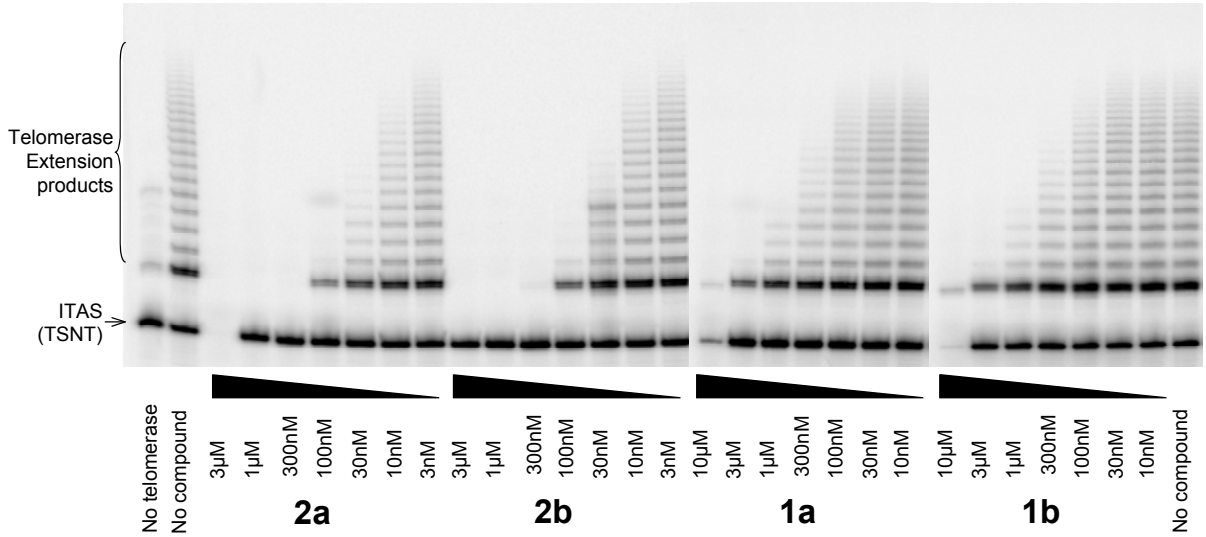

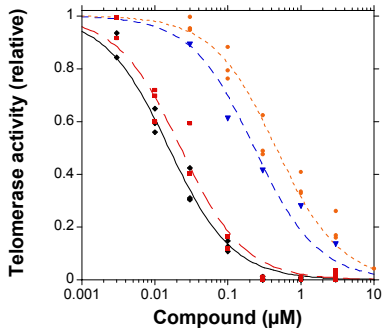

Compound	IC50 ± sd (nM)
2a	16 ± 2
2b	22 ± 3
1a	230 ± 50
1b	460 ± 50

Top: Image of the gel, showing the typical extension ladder obtained after telomerase extension and PCR amplification. Increasing concentrations of compounds lead to a progressive decrease in extension products intensity, while leaving the internal control (ITAS) unaffected, except at very high concentrations.
Bottom: Quantitation of the gel. The relative TRAP activity decreases with increasing ligand concentration. The deduced IC50 are shown on the right.

TRAP assay protocol:
The TRAP reaction was performed in a 20 mM Tris HCl pH 8.3 buffer containing 63 mM KCl, 1.5 mM $MgCl_2$, 1 mM EGTA, 0.005% Tween 20, 0.1mg/ml BSA, 50 µM dTTP, dGTP and dATP, 5 µM dCTP, and the oligonucleotides TS (5'- AATCCGTCGAGCAGAGTT-3') (0.4 µM), ACX (5'-GCGCGGCTTACCCTTACCCTTACCCTAACC-3') (0.4 µM), NT (5'-ATCGCTTCTCGGCCTTTT-3') (0.4 µM) and TSNT (5'-AATCCGTCGAGCAGAGTTAAAAGGCCGAGAAGCGAT-3') (20 fM), 2 units of Taq polymerase, 0.02 mCi/mL of [α^{32}P]-dCTP, 200 ng of A431 CHAPS extracts. After telomerase elongation for 15 minutes at 30°C, 28 cycles of PCR were performed (94°C

30 sec., 50°C 30 sec. and 72°C for 90 sec.). Telomerase extension products were then analysed on a denaturing 7.5 % polyacrylamide, 7M urea 1X Tris Borate EDTA (TBE) vertical gel and exposed to a phosphorimager screen. Extension products were quantified using ImageQuant 5.2 software and normalized to the signal of the extension products without compound.

PCR inhibition on a G4-prone motif:

The PCR control included in a TRAP assay (the so-called ITAS band) is very often used for quadruplex ligands. It demonstrates that the compounds do not interfere with the amplification of a control sequence that is unrelated to the human telomeric motif. However, the observation that the TRAP band is unnaffected does **NOT** demonstrate that the disappearance of the telomeric ladder is the result of a *bona fide* telomerase inhibition. This effect could simply be the result of an inhibition of the amplification of a quadruplex-prone sequence. Binding of a molecule to a quadruplex sequence could well inhibit PCR, as previously shown by Lemarteleur et al. (BBRC, 2004). In order to deconvoluate a true telomerase inhibition from a telomeric amplification inhibition, we performed a PCR assay. In this test, we designed the TS-4r sequence, that mimics a telomerase product containing 4 telomeric motif. No telomerase / cellular extract is added, and we simply compare the PCR amplification of the traditional ITAS (TSNT) sequence with the amplification of this G4-prone sequence.

As shown in the next figure, the TS-4r band disappears at a ≈ 10-fold lower concentration, demonstrating that the PCR amplification of the telomeric motif is selectively affected by compound 2a, with an IC_{50} relatively close to the IC_{50} found in the TRAP assay (especially when comparing the first band of telomerase extension products which corresponds to the addition of 2-4 repeats).

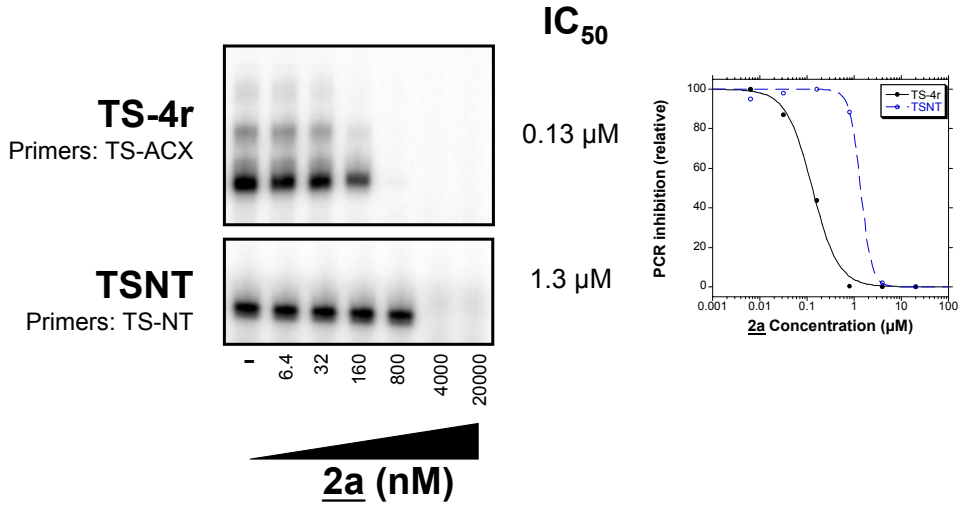

Left: Analysis of PCR products on a gel in the presence of increasing concentrations of compound 2a. *Upper part:* Amplification of a sequence mimicking four repeats of the human telomeric sequence (TS-4r). *Lower part:* Amplification of the TSNT control sequence. The TS-4r sequence is quadruplex-prone, while the TSNT oligonucleotide is unable to form a quadruplex.

Right: Quantitation of the PCR products. The TS-4r band (black) disappears at a lower drug concentration than the TSNT band (in blue).

PCR protocol:

The PCR was performed in the same conditions than TRAP reaction (20 mM Tris HCl pH 8.3 buffer containing 63 mM KCl, 1.5 mM $MgCl_2$, 1 mM EGTA, 0.005% Tween 20, 0.1mg/ml BSA, 50 µM dTTP, dGTP and dATP, 5 µM dCTP, the forward primer TS (5'-AATCCGTCGAGCAGAGTT-3') (0.4 µM), and the reverse primers ACX (5'-GCGCGGCTTACCCTTACCCTTACCCTAACC-3') (0.4 µM) or NT (5'-ATCGCTTCTCGGCCTTTT-3') (0.4 µM)), 2 units of Taq polymerase and 0.02 mCi/mL of [α^{32}P]-dCTP. The DNA template was either TS-4r (5'-AATCCGTCGAGCAGAGTTA**GGG**TTA**GGG**TTA**GGG**TTA**GGG**TT-3') (20 fM) or TSNT (5'-ATTCCGTCGAGCAGAGTTAAAAGGCCGAGAAGCGAT-3') (20 fM). 28 cycles of PCR were performed (94°C 30 sec., 50°C 30 sec. and 72°C for 90 sec.) in the presence of increasing concentrations of compound **2a**. PCR products were then analysed on a denaturing 7.5 % polyacrylamide, 7M urea 1X Tris Borate EDTA (TBE) vertical gel and exposed to a phosphorimager screen. Extension products were quantified using ImageQuant 5.2 software and normalized to the signal of the PCR products without compound.

S12- Dimension & Estimated overlap with quartet:

Data collected form **RCSB Protein Data Bank**
From Parkinson, G. N.; Lee, M. P. H.; Neidle, S. Nature, **2002**, *417*, 876.
Available free of charge at: http://www.rcsb.org/pdb/explore/explore.do?structureId=1KF1

ID: **1KF1** (intramolecular quadruplex ('22-mer'): (d[$AG_3(T_2AG_3)_3$])) - distances evaluated with *WebMol Viewer*

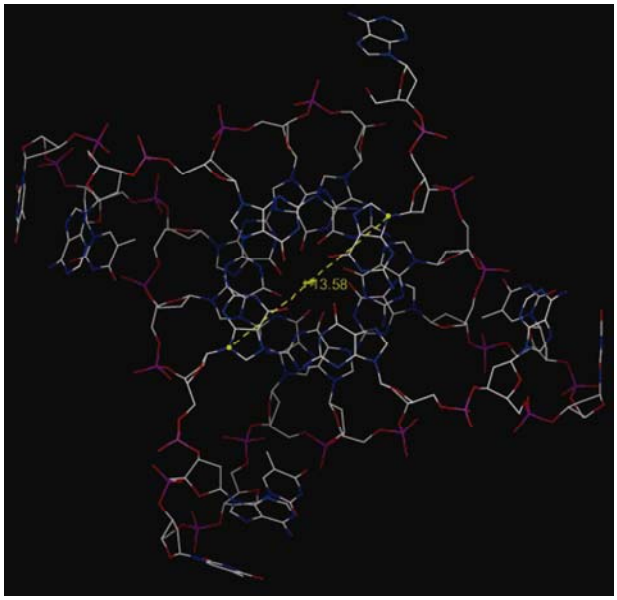

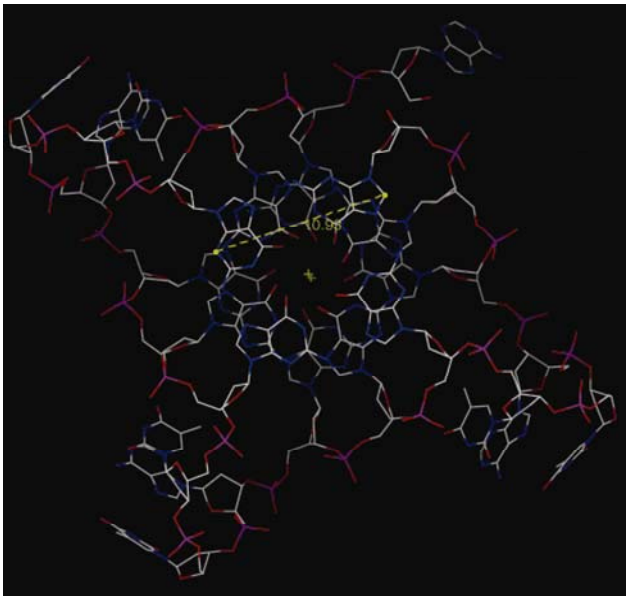

Dimensions & comparison with **2a**:

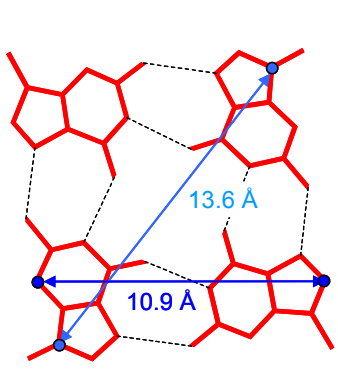

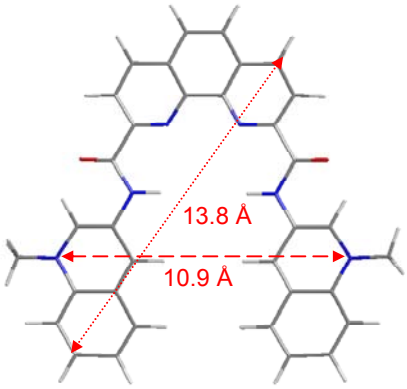

Molecular lengths evaluated after molecular mechanics calculations (MM2, with *Chem3D Ultra 8.0*, CambridgeSoft Crop., MA, USA)